Rapid Communications

Collective enhancement in nuclear level density

G. Mohanto,[*] A. Parihari,[†] P. C. Rout,[‡] S. De, E. T. Mirgule, B. Srinivasan, K. Mahata,[‡] S. P. Behera, M. Kushwaha,[§] D. Sarkar, B. K. Nayak,[‡] and A. Saxena
Bhabha Atomic Research Centre, Mumbai 400085, India

A. K. Rhine Kumar
Department of Physics, Cochin University of Science and Technology, Cochin 682 022, India

A. Gandhi
Department of Physics, Banaras Hindu University, Varanasi 221005, India

Sangeeta
School of Physics and Materials Science, Thapar Institute of Engineering and Technology, Patiala-147004, Punjab, India

Nabendu K. Deb
Department of Physics, Gauhati University, Guwahati, Assam 781014, India

P. Arumugam
Department of Physics, Indian Institute of Technology Roorkee, Uttarakhand 247 667, India

(Received 14 March 2019; revised manuscript received 18 June 2019; published 24 July 2019)

Several experimental investigations have reported evidence of collective enhancement of the nuclear level density and its fadeout. However, a suitable method is needed for experimental determination of the enhancement factor as a function of excitation energy. In this study, neutron spectra were measured in coincidence with evaporated α particles produced in the reactions ^{11}B + ^{181}Ta, ^{197}Au. The nuclear level density parameter has been extracted for the Os ($A \approx 188$) and Pb ($A \approx 204$) isotopes by comparing neutron spectra with statistical model prediction. Evidence for collective enhancement has been found for Os nuclei whereas no such enhancement has been seen for Pb nuclei. The energy-dependent enhancement factor has been extracted by simultaneous fitting of the neutron spectra at various excitation energies. Near a temperature of 0.8 MeV, the enhancement starts to fadeout which is lower than the theoretically predicted temperature of 1.4 MeV for ^{187}Os. Also, free energy surface calculation shows that the ^{187}Os nucleus undergoes a transition from collective prolate to noncollective oblate shape close to the temperature of 0.8 MeV, corroborating the early fadeout. No such shape transition is seen for ^{203}Pb.

DOI: 10.1103/PhysRevC.100.011602

The properties exhibited by atomic nuclei are a manifestation of either its single-particle nature or collective degrees of freedom and the interplay between the two. Nuclear level density is one such physical quantity where the single-particle and collective natures coexist [1–3]. The nuclear level density for a spherical nucleus with excitation energy U and angular momentum J is given by [2,4]

$$\rho(U,J) = \frac{2\pi(2J+1)}{\sqrt{8\pi}\sigma^2} \exp\left\{-\frac{J(J+1)}{2\sigma^2}\right\}\rho(U). \quad (1)$$

Here σ is the spin cutoff factor and $\rho(U)$ is the total number of levels at an energy U. For a deformed nucleus, depending on the level of symmetry, each intrinsic state gives rise to rotational bands which enhances the level density over that of a spherical nucleus. This enhancement is of the order of σ^2 for an axially deformed nucleus rotating about an axis perpendicular to the symmetry axis and of the order of σ^3 for nuclei with no rotational symmetry. As the degree of rotational symmetry increases, the enhancement is destroyed. Similarly, vibrational collectivity can also cause enhancement in the level density but the magnitude is small compared to the rotational enhancement [2,5,6]. At sufficiently higher temperature no distinction can be made between rotational

[*]gayatrimohanto@gmail.com
[†]Present address: Inter University Accelerator Centre, New Delhi 110067, India.
[‡]Homi Bhabha National Institute, Anushaktinagar, Mumbai 400094, India.
[§]Department of Physics, University of Mumbai, Mumbai 400098, India.

and intrinsic motion and the level density approaches that of a spherical nucleus. The temperature T_{cr} where this transition takes place was shown to be $T_{cr} \approx 40\beta_2 A^{-\frac{1}{3}}$ by Björnhom *et al.* [2], β_2 and A being the deformation and mass of the nucleus, respectively.

Experimental evidence of the collective enhancement of level density (CELD) and its fading out was observed by Jhungans *et al.* [7] in a fragmentation study of heavy nuclei. However, a later study of evaporated α-particle spectra showed no evidence of fadeout [8] for the compound nucleus (CN) ^{178}Hf over the excitation energy range 54–124 MeV. More recently, evaporated neutron spectra from CN in the excitation energy range 27–37 MeV have shown evidence of fadeout of collective enhancement [9,10]. This indicates that neutron spectra are useful tools for experimental investigation of CELD and its fadeout.

Populating CN in the excitation energy range 20–40 MeV is difficult through heavy ion fusion reactions, and light ion induced reactions may bring in contamination from pre-equilibrium emission. Transfer reactions are often used to populate low excitation energy in the composite system [11]. In the present study we have measured evaporated neutrons in coincidence with evaporated α particles for two reactions ^{11}B + ^{181}Ta, ^{197}Au populating CN ^{192}Pt and ^{208}Po, respectively. The level density parameter as a function of energy has been extracted by comparing experimental n spectra with statistical models which showed signature of collective enhancement.

The experiment was carried out at the BARC-TIFR Pelletron LINAC facility, Mumbai, using the 14UD Pelletron accelerator. Pulsed beam of ^{11}B was accelerated to bombard self-supporting targets of ^{181}Ta and ^{197}Au, at energies 61.5 and 63.0 MeV, respectively. Two ΔE-E telescopes consisting of large area silicon strip detectors (50 × 50 mm^2 with 16 strips) were placed at $\pm 150^\circ$ to detect the evaporated charged particles. The thickness of ΔE and E detectors were 54 and 1500 microns, respectively. To detect neutrons, 14 liquid scintillator detectors were placed at a distance of 72 cm from the target covering an angular range from 58° to 143° with respect to the beam direction. The time of flight of neutrons with respect to the beam pulsing RF signal was recorded. The pulse shape discrimination (PSD) property of liquid scintillators was exploited for differentiating between neutrons and γ rays.

The α-particle spectra obtained for both the reactions were compared with statistical model prediction using the code PACE [12]. It was observed that experimental α-particle spectra were well reproduced with statistical model calculations with inverse level density parameter values $k = 11.5$ and 10.5 for ^{11}B + ^{197}Au and ^{11}B + ^{181}Ta, respectively. Good agreement between the experimental α-particle spectra and statistical model prediction suggests that the detected α particles are from CN evaporation.

The energy of the neutron (E_n) was determined using the time of flight technique. The neutron spectra were obtained corresponding to various α-particle energy (E_α) bins of 1 MeV width in the energy range of 20.5–29.5 MeV. In order to estimate the probability of first chance α-particle evaporation, i.e., α particles evaporated before any neutron emission, detailed

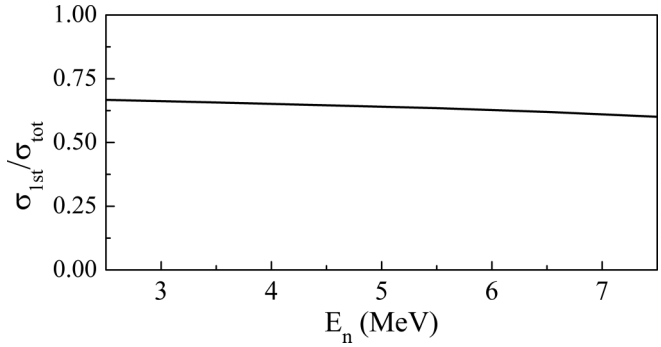

FIG. 1. Statistical model prediction of the ratio of σ_{1st} (first chance α-particle gated neutron cross section) to the σ_{tot} (total α-particle gated neutron cross section) as a function of neutron energy E_n for α-particle energy of 25 MeV for the reaction ^{11}B + ^{181}Ta.

calculation of αxn channels were performed using a statistical model code [13]. These calculations show that probability of first chance α-particle evaporation increases with increase in E_α. In the neutron energy range of 2.5–7.5 MeV, this contribution is ≈50% for the lowest E_α bin used in this study and ≈80% for the highest E_α bin. Figure 1 shows the ratio of first chance α-particle gated neutron cross section (σ_{1st}) to the total α-particle gated neutron cross section (σ_{tot}) as a function of E_n for the reaction ^{11}B + ^{181}Ta at $E_\alpha = 25$ MeV. It can be seen from Fig. 1 that for the E_n variation from 2.5 to 7.5 MeV, the slopes of the first chance α-particle gated neutron spectra can have ≈12% variation due to the contribution of the neutrons that are evaporated before α particles. This 12% change in the slopes of the neutron spectra can result in a systematic reduction of 0.5 in the extracted k values, which is within the uncertainty limit. The excitation energy (E^*) of the residual nuclei ^{188}Os and ^{204}Pb, after one α-particle evaporation, was determined by subtracting the α-particle kinetic energy and the separation energy from the CN excitation energy (E^*_{CN}). Neutron spectra for four different E^* values are shown in Fig. 2. Statistical model calculations were performed by varying the inverse level density parameter k to obtain best fit for

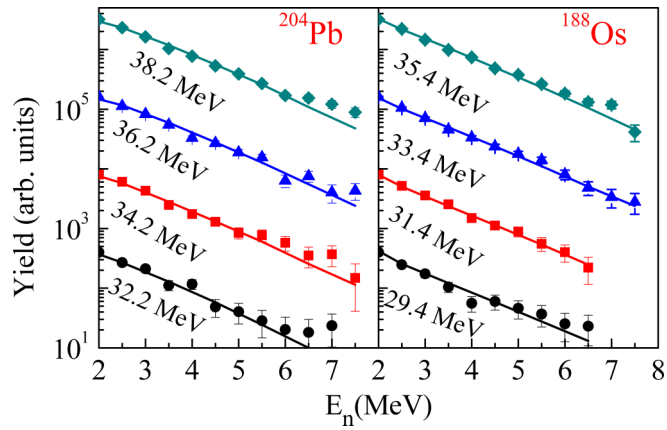

FIG. 2. Experimental neutron spectra for residual nuclei ^{204}Pb and ^{188}Os. Solid lines show statistical model calculation using best fitted k values.

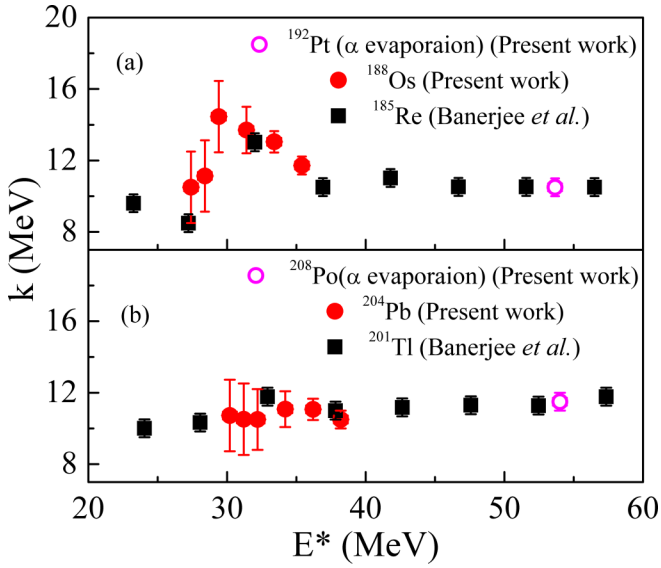

FIG. 3. Inverse level density parameters as a function of excitation energy extracted from reactions ^{11}B + ^{181}Ta, ^{197}Au. The k parameters obtained from α-particle spectra are shown by open circles, and results from Banerjee *et al.* [9] are shown by filled squares.

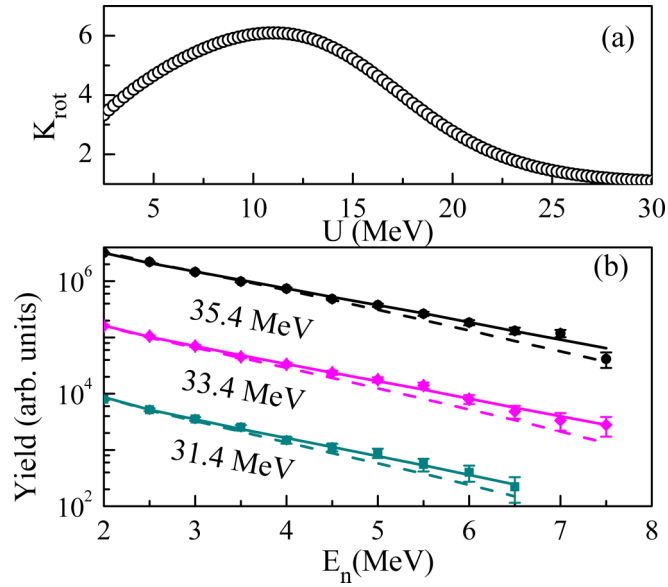

FIG. 4. (a) Energy-dependent collective enhancement factor obtained from simultaneous fitting of the neutron spectra. (b) Neutron spectra evaporated from ^{188}Os. Statistical model calculation using an enhanced level density are shown by solid lines and calculation without enhancement are shown by dashed lines. Excitation energies of evaporating nucleus are given with each spectrum.

both the residual nuclei at various energies. The calculated neutron spectra are shown in Fig. 2 by solid lines and the corresponding k values are shown as a function of E^* in Fig. 3. The k values obtained from evaporated α-particle spectra for the compound nuclei ^{192}Pt and ^{208}Po are also shown in this figure by open circles. The inverse level density parameter obtained from neutron evaporation for neighboring CN ^{185}Re and ^{201}Tl reported by Banerjee *et al.* [9], are shown in the same figure (solid squares) for comparison and good agreement between the k values obtained from different experimental methods can be seen. For the decay of ^{204}Pb, the k parameter remains constant over the energy range studied in the present work, whereas for the decay of ^{188}Os, the k value shows a peak-like structure in the excitation energy range 28–35 MeV. The occurrence of such deviation was reported by Banerjee *et al.* [9] and attributed to the fading out of CELD in deformed nuclei. The fadeout of collective enhancement will result in a change in the slope of the level density which will be reflected in the evaporated particle spectra when the intrinsic excitation energy of daughter nuclei fall in the energy range of fadeout. Neutrons which are evaporated from ^{188}Os will populate the daughter nucleus in the low excitation energy range (13–27 MeV) where fadeout of CELD is predicted [2,5,9,14]. The nuclei in the decay chain of ^{188}Os (^{185,186,187}Os) are highly deformed ($\beta_2 = 0.21$–0.23) [15] causing rotational collectivity to enhance the level density. On the other hand, nuclei in the decay chain of ^{204}Pb are nearly spherical and as expected, no variation in k value is observed for ^{204}Pb decay in this energy range. It can be mentioned here that neutrons which are evaporated before α-particle evaporation will populate daughter nuclei at higher excitation energy (37–42 MeV) where the shape of the nuclei is predicted to be spherical and will not have any change in the neutron spectra due to fadeout of CELD.

In order to investigate the origin of energy dependence of k for ^{188}Os in more detail we have performed statistical model calculations including collective enhancement in level density. Phenomenologically, the total nuclear level density can be expressed as [3]

$$\rho(U) = \rho_{\rm int}(U) * K_{\rm coll}(U)\,, \tag{2}$$

where, $K_{\rm coll}(U)$ is the collective enhancement factor and $\rho_{\rm int}(U)$ is the intrinsic level density. $K_{\rm coll}(U)$ $[= K_{\rm rot}(U)K_{\rm vib}(U)]$ has two components: rotational $[K_{\rm rot}(U))]$ and vibrational $([K_{\rm vib}(U)]$. Since, the residual nuclei in the decay chain of ^{188}Os are highly deformed it is expected that $K_{\rm rot}$ would be much larger than 1 whereas $K_{\rm vib} \approx 1$ except for very low energy [5,14]. This enables us to consider $K_{\rm coll} \approx K_{\rm rot}$. In the present analysis the form of the rotational enhancement factor as given by Hansen *et al.* [5] was taken,

$$K_{\rm rot} = (\sigma_\perp^2 - 1) f(U) + 1\,, \tag{3}$$

$$f(U) = \frac{1}{1 + \exp[(U - U_{\rm crit})/d_{\rm crit}]}\,. \tag{4}$$

Where $\sigma_\perp$ is the spin cutoff parameter perpendicular to the symmetry axis which can be written as $\sigma_\perp^2 = \frac{\Im_\perp T}{\hbar^2} \approx 0.01389 A^{\frac{5}{3}}(1 + \beta_2/3)\sqrt{\frac{U}{a}}$, $\Im_\perp$ being the rigid body moment of inertia perpendicular to the symmetry axis, A is the mass number of the nucleus, T is temperature, and $a = A/k$ the level density parameter. The amplitude of the enhancement was varied as a parameter and $\sigma_\perp^2$ in Eq. (3) was replaced by $\alpha_1\sqrt{\frac{U}{a}}$, with α_1 being treated as a parameter. The shape of the enhancement factor depends on two critical parameters, $U_{\rm crit}$

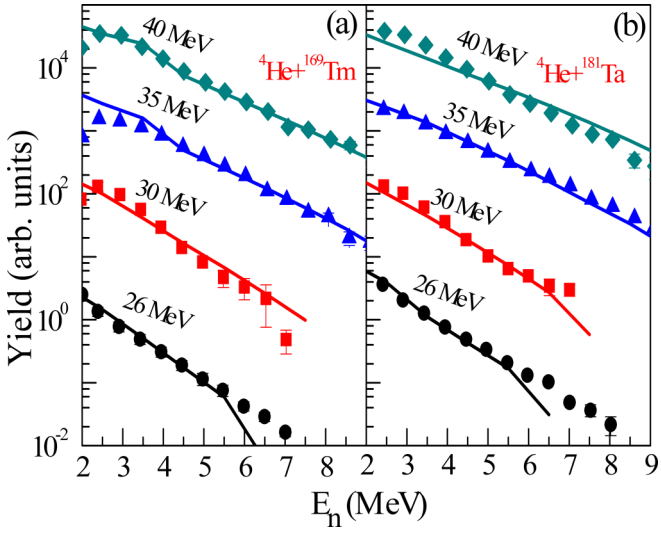

FIG. 5. Neutron spectra for reactions ^{4}He + ^{169}Tm, ^{181}Ta (data taken from [9]) along with statistical model calculations (shown by lines). Beam energies are mentioned with each spectra.

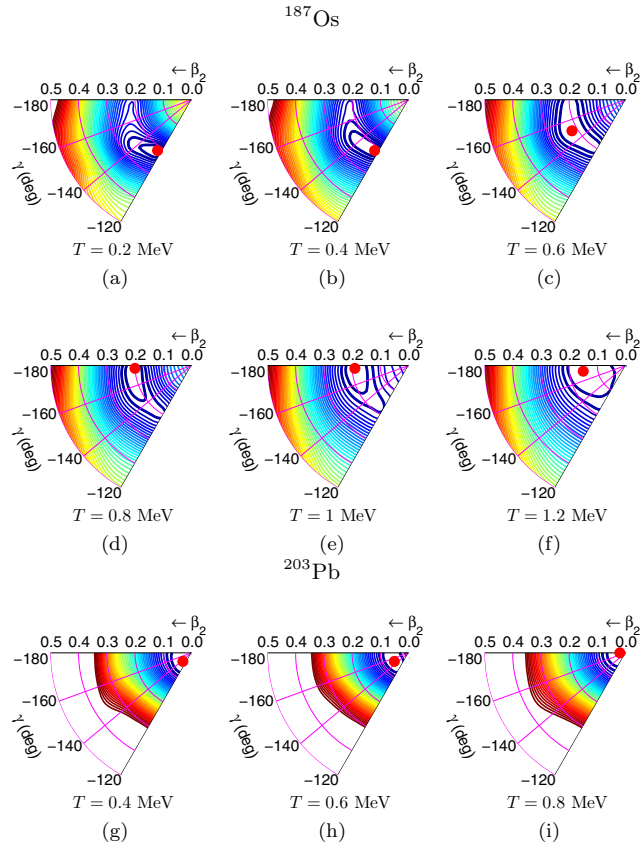

FIG. 6. Free energy surfaces (FESs) of ^{187}Os and ^{203}Pb at different temperatures (T). In this convention, $\gamma = 0°$ and $-120°$ represent noncollective and collective prolate shapes, respectively, and $\gamma = -180°$ and $-60°$ represent the noncollective and collective oblate shapes, respectively. The line spacing of each contour is 0.2 MeV. The most probable shape (MPS) is shown by a filled circle.

and $d_{\rm crit}$. These two parameters along with α_1 were varied to obtain simultaneous best fit for all the neutron spectra at different excitation energies using a fixed k value. It was observed that different combinations of α_1, $U_{\rm crit}$, and $d_{\rm crit}$ could reproduce the neutron spectra at a particular excitation energy of the evaporating nuclei. However, the same combination was unable to explain the spectra at other excitation energies and simultaneous fitting of the neutron spectra over the entire excitation energy range was necessary to obtain the correct set of parameters. The value of k (=10.5 for ^{188}Os) was taken from a higher excitation energy region where k shows little variation. The values of the best fit parameters were $\alpha_1 = 9.0 \pm 2.0$ and $U_{\rm crit} = 16.0 \pm 2.0$, $d_{\rm crit} = 3.0 \pm 1.0$ and the corresponding enhancement factor as a function of energy is shown in Fig. 4(a). The maximum enhancement was found to be ≈6, which is of similar order to the maximum value calculated using the shell-model Monte Carlo approach for Sm isotopes [14]. This enhancement factor is significantly less than the predicted value of $\sigma_\perp^2$. This is because the emission spectra for low spin region are dominated by state density rather level density [4], causing the enhancement to be $\sqrt{2/\pi}\sigma_\perp$ instead of $\sigma_\perp^2$. The extracted collective enhancement factor shows a maximum near $U = 12$ MeV and then decreases. The value of the critical energy (or temperature) for fadeout is found to be smaller than the critical values predicted by Hansen *et al.* ($U_{\rm crit} = 120\beta_2 A^{\frac{1}{3}} \approx 30$ MeV) [5] as well as Björnhom *et al.* ($T_{\rm crit} \approx 1.4$ MeV; $U_{\rm crit} \approx 35$ MeV) [2] indicating that fadeout is taking place at a lower energy than predicted.

The calculated neutron spectra with inverse level density parameter $k = 10.5$ successfully reproduced the experimental neutron spectra for ^{11}B + ^{181}Ta after inclusion of rotational enhancement and these are shown in Fig. 4(b) by solid lines. Dashed lines show calculation with the same k value without inclusion of rotational enhancement. It is seen from Fig. 4(b), that inclusion of collective enhancement in the nuclear level density gives better fit of the experimental data with $k = 10.5$ for all the energies. This suggests that the peak like structure in k values for ^{11}B + ^{181}Ta decay [Fig. 3(a)] is due to noninclusion of the CELD in the statistical model calculation.

The same enhancement factor $K_{\rm rot}(U)$ was used to calculate the neutron spectra for the reactions ^{4}He + ^{169}Tm, ^{181}Ta, reported by Banerjee *et al.* (Fig. 5) to investigate the mass and deformation dependence of collective enhancement. The k values (9.5 for ^{4}He + ^{169}Tm and 10.5 for ^{4}He + ^{181}Ta) used for these calculations correspond to those of the higher energy region. It can be seen from Fig. 5 that all the neutron spectra are well reproduced by the present collective enhancement factor. It can be noticed that the same collective enhancement explains the decay of ^{173}Lu (^{4}He + ^{169}Tm), ^{185}Re (^{4}He + ^{181}Ta), and ^{188}Os. This indicates that fadeout of the collective enhancement factor ($U_{\rm crit}$ and $d_{\rm crit}$) does not depend strongly on mass and/or ground-state deformation contrary to the suggestion by Hansen *et al.* [5]. Similar observations were reported by Jhungans *et al.* [7] where deformation-independent damping of collective enhancement was needed to explain the experimental results.

A microscopic-macroscopic calculation of free energy surface (FES) (shown in Fig. 6) for nuclei ^{187}Os and ^{203}Pb,

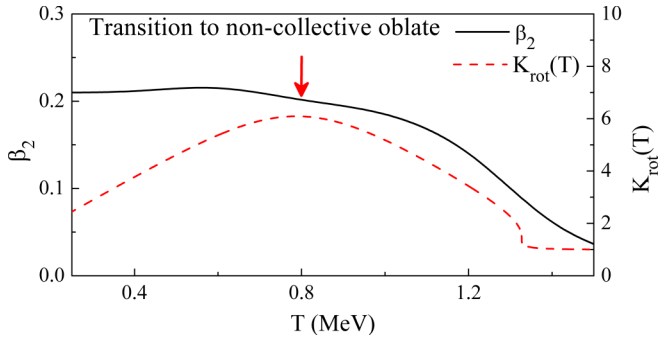

FIG. 7. β_2 (scale shown on left axis) corresponding to the most probable shape of ^{187}Os as a function of temperature is presented by solid line. Collective enhancement factor (scale shown on right axis) obtained from present measurement as a function of temperature is also shown in the same plot by dashed line. Temperature where the nucleus becomes oblate is indicated by an arrow.

populated after one neutron evaporation from nuclei ^{188}Os and ^{204}Pb respectively, has been carried out to study the evolution of collectivity in the nucleus as a function of temperature. The pairing correlations are incorporated in the free energy calculations through the BCS approach [16,17]. According to the convention used in the present calculation [18], $\gamma = 0^\circ$ and -120° represent noncollective (rotation of the nucleus is about the symmetry axis) and collective (axis of rotation is perpendicular to the symmetry axis of the nucleus) prolate shapes, respectively, and $\gamma = -180^\circ$ and -60° represent the noncollective and collective oblate shapes, respectively. The contour line spacing is 0.2 MeV. The most probable shape (MPS) is represented by a filled circle and the first two minima are represented by thick lines. As the temperature T increases, the MPS of the nucleus ^{187}Os, denoted by the red dot in Figs. 6(a)–6(f), shows a transition from the prolate to the oblate shape. At $T = 0.2$ and 0.4 MeV, the MPS of the nucleus corresponds to a collective prolate minimum with an axial deformation $\beta_2 = 0.21$ and $\gamma = -120^\circ$. But, the FES shows a crisp minimum at $T = 0.4$ MeV. As the temperature increases to $T = 0.6$ MeV the nucleus shows a clear γ softness with the MPS at $\beta_2 = 0.21$ and $\gamma = -150^\circ$, representing a triaxial shape. With increase in temperature ($T = 0.8$ and 1 MeV) the MPS of the nucleus shows a noncollective oblate shape with $\beta_2 = 0.2$ and $\gamma = -180^\circ$. At $T = 1.2$ MeV the nucleus shows a decrease in the deformation with $\beta_2 \approx 0.15$ and $\gamma \approx -180^\circ$ and the first two minima span a smaller deformation area. As the T increases, the nucleus shows a decrease in the deformation and the equilibrium shape becomes spherical. ^{203}Pb on the other hand is spherical or nearly spherical [Figs. 6(g)–6(i)] at all temperatures.

The axial deformation value (β_2) for ^{187}Os corresponding to MPS at different temperatures are shown in Fig. 7 along with the extracted $K_{\rm rot}$ as a function of temperature. It is clear from the figure that the fadeout of collective enhancement starts at a temperature where the nucleus undergoes a transition from collective prolate ($\gamma = -120^\circ$) to a noncollective oblate ($\gamma = -180^\circ$) and vanishes at a temperature where the shape becomes spherical.

In summary, evaporation neutron spectra have been measured in coincidence with evaporated α particles for CN ^{192}Pt and ^{208}Po. The level density parameter has been obtained by fitting the experimental neutron spectra with statistical model prediction. A peak-like structure in the inverse level density parameter as a function of excitation energy was observed for the reaction ^{11}B + ^{181}Ta, whereas no significant change was observed for ^{11}B + ^{197}Au. This structure was attributed to fadeout of CELD. Consequently, the energy-dependent collective enhancement factor was obtained from statistical model analysis of the measured neutron spectra. The derived enhancement factor starts to fadeout near 12 MeV of excitation energy and vanishes beyond 25 MeV, which is smaller than the predicted fadeout energy values [2,5]. Critical parameters of the enhancement did not show any significant dependence with mass and/or deformation over the studied mass region. Free energy surface calculation for the nuclei ^{187}Os shows collective prolate ($\gamma = -120^\circ$) to noncollective oblate ($\gamma = -180^\circ$) shape transition at $T = 0.8$ MeV which is consistent with our experimental observation. FES calculation for ^{203}Pb shows nearly spherical shape over the studied energy range which is in agreement with the energy-independent k value. This result will be helpful in furthering our understanding of the statistical properties of atomic nuclei.

We thank D. R. Chakrabarty for providing the code for detailed calculation of αxn channel cross sections and various scientific discussion. We thank V. M. Datar and R. K. Choudhury for their interest in the present work and their valuable suggestions. We thank the staff of Pelletron Linac Facility for providing good quality beams throughout the experiment. A.K.R.K. acknowledges the financial support provided by the Department of Science and Technology (DST), India, via the DST-INSPIRE Faculty award.

[1] A. Bohr and B. Mottelson, *Nuclear Structure,* Vol. II (Benjamin, Reading, MA, 1975).
[2] S. Björnholm, A. Bohr, and B. Mottelson, *International Conference on the Physics and Chemistry of Fission, Vol. 1 Rochester, New York, 1973* (IAEA, Vienna, 1974), pp. 367–374.
[3] A. V. Ignatyuk, K. K. Istekov, and G. N. Smirenkin, Sov. J. Nucl. Phys. **29**, 450 (1979).
[4] S. M. Grimes, Phys. Rev. C. **78**, 057601 (2008).
[5] G. Hansen and A. Jensen, Nucl. Phys. A **406**, 236 (1983).
[6] A. Koning, S. Hilaire, and S. Goriely, Nucl. Phys. A **810**, 13 (2008).
[7] A. Junghans, M. de Jong, H.-G. Clerc, A. Ignatyuk, G. Kudyaev, and K.-H. Schmidt, Nucl. Phys. A **629**, 635 (1998).
[8] S. Komarov, R. J. Charity, C. J. Chiara, W. Reviol, D. G. Sarantites, L. G. Sobotka, A. L. Caraley, M. P. Carpenter, and D. Seweryniak, Phys. Rev. C **75**, 064611 (2007).
[9] K. Banerjee, P. Roy, D. Pandit, J. Sadhukhan, S. Bhattacharya, C. Bhattacharya, G. Mukherjee, T. Ghosh, S. Kundu, A. Sen, T. Rana, S. Manna, R. Pandey, T. Roy, A. Dhal, M. Asgar, and S. Mukhopadhyay, Phys. Lett. B **772**, 105 (2017).

[10] D. Pandit, S. Bhattacharya, D. Mondal, P. Roy, K. Banerjee, S. Mukhopadhyay, S. Pal, A. De, B. Dey, and S. R. Banerjee, Phys. Rev. C **97**, 041301(R) (2018).
[11] P. C. Rout, D. R. Chakrabarty, V. M. Datar, S. Kumar, E. T. Mirgule, A. Mitra, V. Nanal, S. P. Behera, and V. Singh, Phys. Rev. Lett. **110**, 062501 (2013).
[12] A. Gavron, Phys. Rev. C. **21**, 230 (1980).
[13] D. R. Chakrabarty (private communication).
[14] C. Özen, Y. Alhassid, and H. Nakada, Phys. Rev. Lett. **110**, 042502 (2013).
[15] P. Moller and J. Nix, At. Data Nucl. Data Tables **59**, 185 (1995).
[16] A. K. Rhine Kumar, P. Arumugam, and N. D. Dang, Phys. Rev. C **90**, 044308 (2014).
[17] A. K. Rhine Kumar, P. Arumugam, and N. D. Dang, Phys. Rev. C **91**, 044305 (2015).
[18] A. K. Rhine Kumar and P. Arumugam, Phys. Rev. C **92**, 044314 (2015).